Data and Queueing Analysis of a Japanese Arrival Flow

C. Gwiggner, A. Kimura, S. Nagaoka
Electronic Navigation Research Institute
Chofu, Tokyo
[claus,kimura,nagaoka]@enri.go.jp

Abstract: We analyze the east-bound arrival flow to Tokyo International Airport. Currently, aircraft are vectored in the en-route sector that is adjacent to the approach area, in order to meet a metering constraint. These vectors take place largely during the descent phase. In the future, arrival traffic shall be 'synchronized' in the cruise phase for less controller workload and more fuel efficiency. Our results are a good correspondence between a simple queueing model and empirical data, low average delays, and high prediction uncertainties of sector crossing times. This allows to identify strategies for future traffic synchronization that are tailored to the Japanese airspace.

Keywords: Air Traffic Flow Management, Radar data, Queueing analysis

1. INTRODUCTION

Arrival management at busy airports often starts already in the en-route sectors adjacent to the approach area [1]. For example, at Tokyo International Airport, traffic enters the approach area from three directions at predefined metering rates. These rates assure that the merging of the flows can be done efficiently. But in today's practice, metering the flows en-route creates high controller workload and fuel inefficient trajectories. In the future, traffic management coordinators (TMC) need strategies to synchronize arrival traffic for more efficient queue management [2, 3].

For this, they need to estimate roughly (in the order of minutes) how much and when to delay flights in the upstream sectors to the arrival by speed control and vectoring. The higher the altitude of a delay maneuver, the more fuel efficient generally it is. On the other hand, predictions over long time horizons introduce uncertainties (e.g. certain aircraft will still be on the ground). Since the aim of arrival management is to use the runway capacity as efficiently as possible, such uncertainties create a risk of under-usage of runway capacity.

Related work identifies relationships between ATFM and en-route delays [4] and decision support tools for traffic management coordinators [5, 6]. The drawback of such tools is that they do not give any guarantees that their calculations are applicable. For example, how much airspace is necessary to absorb the predicted delays ? Or what is the maximum delay that such a tool predicts ? The innovation in our research is that we analyze the concept and the limitations of the distribution of en-route delays between several sectors. In this article, we analyze the east-bound arrivals to Tokyo International Airport, the largest of the Japanese arrival flows.

The paper contains three parts: In the next section we give a characterization of the traffic flow. The following part is an queueing analysis of delays. The last part discusses speed control, the simplest of all traffic synchronization strategies.

2. DATA ANALYSIS

At Tokyo Int'l Airport, which is one of the busiest airports in Asia, traffic enters the approach area through three gates; one one from the South, one from the West and one from the North. On a normal day about 450 flights arrive at the airport, 70% from the South and the West, and 30 % from the North. Usually, one runway is available exclusively for landings.

There are two main reasons for arrival delays:

- Metering constraints at the entry gates
- Merging of flows inside the approach area

In order to protect the approach area from congestion, aircraft are separated by 10 NM on the West and North gates, and 20 NM on the South gate. This is larger than the usual 5 NM separation, so delays have to be expected. In the remainder we call such delays *metering delays*. Once the aircraft entered the terminal area, the three flows are merged into one. Delays may occur here, as well.

In this paper we analyze the West gate because it creates the highest metering delays. The West gate lies inside the en-route sector T09, belonging to the Tokyo Area Control Center. The size of T09 is approximately 150 NM x 60 NM. We selected 10 days of 'normal' traffic from the months August, October and December 2008, i.e., where no exceptional events or delays were reported. We removed outliers by hand (about 10 % of missing or erroneous fields in the source data), leaving us with n=2816 flights. On a typical day, about 450 aircraft per day enter it, and about 290 of them are arrivals to Tokyo Int'l Airport. The main tasks for the controllers in T09 are to meter the aircraft at the gate, and to supervise the crossing of the other ones.

Aircraft enter the sector on six different routes and leave the sector at the metering point, which is located at the boundary between the en-route airspace and the terminal area. The in-flight altitudes are between FL 200 and FL 410, but the outflow occurs on flight level 160. This means that the top of descent (tod) lies inside T09.

Table 1: Average western arrival flow to Tokyo Int'l airport (T09).

Origin	**Flights**	FL_{in} **(ft)**	v_{in} **(kt)**	FL_{out} **(ft)**	v_{out} **(kt)**	**rate** (min^{-1})
Central	137 (49 %)	291 (54)	484 (39)	155 (14)	379 (28)	0.15
South	129 (46 %)	357 (44)	507 (39)	157 (16)	382 (29)	0.15
Int'l	13 (5 %)	372 (37)	522 (35)	156 (14)	378 (25)	0.02

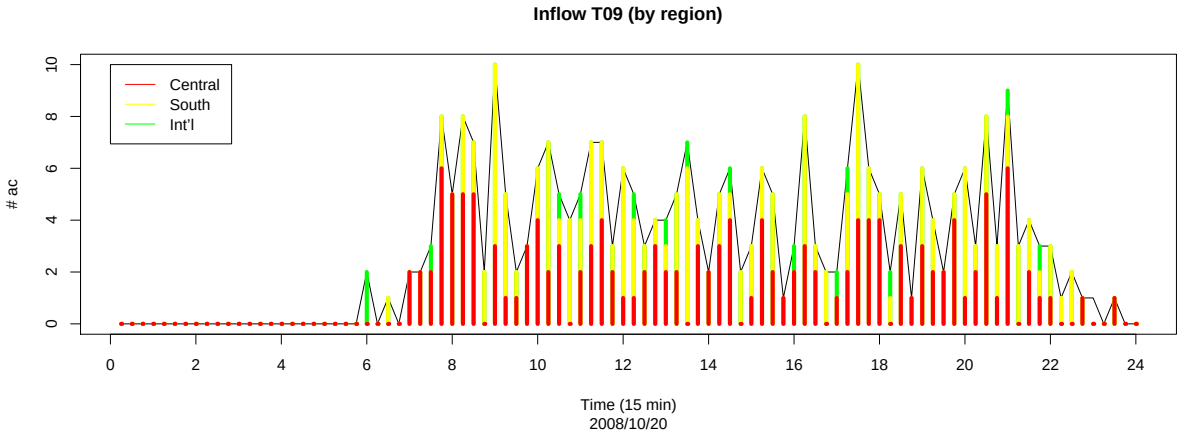

Figure 1: Inflows into T09 by region.

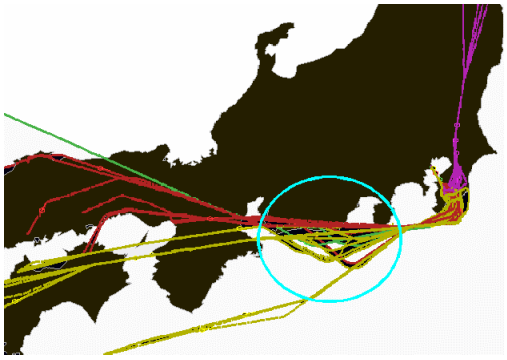

Figure 2: Lateral inefficiencies.

We grouped the origins of the arriving aircraft into three regions: 1: Central Japan (Osaka area and western Honshu), 2: South Japan (Kyushu Island), 3: International flights (China, Korea). Figure 1 shows the numbers of aircraft entering the sector over time. We counted them in slots of size 15 minutes. The three colors represent the three different regions. One can see fluctuating demand around a value of 5 aircraft per slot. Peak hours (morning and evening) are not clearly visible, but from background knowledge it can be expected that in the morning and evening hours, a slightly higher demand exists than during the day.

Properties of the flows per region can be seen in Table 1. Aircraft arrive roughly in equal number from Central and South Japan, and only 5% of the flights are international (column 2). Flights from Central Japan arrive in average on a lower flight level (FL 291) than those from South Japan (FL 357) or international (FL 372) (column 3). The numbers in parentheses are the standard deviations in the corresponding units. The average ground speed at the sector entry grows with the flown distance, increasing from 484 kt, over 507 kt to 522 kt (column 4). At the sector exit, the average speed is equally about 380 kt with 27 kt standard deviation, on flight level 156 (columns 5,6). For a typical day, the inflow rates for the three regions are about 0.15 (ac/min) for the regions 1 and 2 and 0.02 (ac/min) for the international flights (column 7). The total arrival rate is about 0.32 aircraft per minute. The capacity at the metering point is given by a $s_m = 10$ NM spacing requirement. Given the average ground speed of the flow of $\bar{v}_{out} = 363kt$, this translates into $\mu = \bar{v}_{out}/s_m = 0.61$ (ac/min).

The inefficiencies due to vectoring can be seen in Figure 2. Aircraft enter T09 from the West, and are visibly deviated from their shortest paths (cyan circle). After leaving the sector, they turn left to towards the final approach. Again, delays may occur because of merging.

3. METERING DELAYS

The flow management center, located in Fukuoka, continuously monitors the demand and capacity of the airspace. If an imbalance is detected, typical measures like ground delays and miles-in-trail, or more recent ones like arrival slot swappings can be taken. By experience,

the flow managers only attribute ground delays larger than 10 minutes. Lower delays have to be absorbed during the flight, for example by arrival vectors. The justification for this practice is that wind and other operational uncertainties make exact trajectory predictions difficult. The drawback is that, when by chance too many aircraft arrive at the terminal area at the same time, large en-route delays occur. This creates fuel inefficiency and high controller workload.

In this section we analyze the en-route metering delays. The purpose of the analysis is to quantify them. In the next section, we use these results to discuss future strategies for more fuel efficient arrival flows. We start with the following definition:

Definition (Metering Delay)
The difference between estimated and scheduled time of arrival at a metering point due to a metering constraint. The estimated time of arrival is the arrival time without controller intervention. The scheduled time of arrival is the time due to controller intervention, such as speed control or vectoring.

3.1 Theoretical Metering Delays

In theory, a metering delay can be explained as follows: Let $(eta_1, ..., eta_n)$ be the the estimated arrival times of the aircraft at the metering point, and $m_i = s_m/v_i$ (min) the metering constraint. We express m_i here as a time, using the ground speed v_i of aircraft i, but other expressions, for example based on the average speed of all aircraft, are possible. Aircraft i will have left the metering point s_m NM behind at time $tl_i = w_i + eta_i + m$, where w_i is its metering delay. If aircraft $i+1$ is estimated to arrive before tl_i, its metering delay will be $w_{i+1} = tl_i - eta_{i+1} = w_i - (eta_{i+1} - eta_i) + m_i > 0$. If it is estimated to arrive after tl_i, its metering delay will be 0. Thus:

$$w_{i+1} = max(w_i - (eta_{i+1} - eta_i) + m_i, 0), \qquad (1)$$

with $i \geq 1$, and $w_1 = 0$.

Equation (1) is the natural delay relation in queueing theory [7]. Although there are fundamental results in the theory of queues, except for simple cases, the delay distributions are difficult to obtain [8]. On the other hand, results for the average delays are known. In the general case, the only assumptions on the variables in equation (1) are that $a_i = eta_i - eta_{i-1}$ and m_i are sequences of independent but identically distributed random variables with distribution functions A and M. Their means are $1/\lambda$ (min) and $1/\mu$ (min) and their variances are $\sigma_i^2, i \in \{A, B\}$. Then, tedious but basic operations lead to the following upper bound for the equilibrium average delay

$$E(W) \leq \frac{\lambda(\sigma_A^2 + \sigma_M^2)}{2(1-\rho)}, \qquad (2)$$

where $\rho = \lambda/\mu$ is the system usage and $E(.)$ is the expected value of its argument. In the special case of a Poisson arrival flow, it is known that the bound gets strict to

$$E(W) = \frac{\lambda E(M^2)}{2(1-\rho)}, \qquad (3)$$

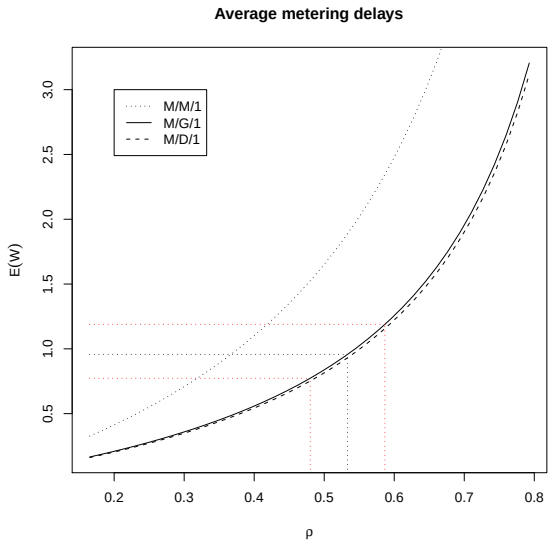

Figure 3: Average theoretical metering delays.

where $E(M^2) = \sigma_M^2 + 1/\mu^2$ [7]. For deterministic service, the variance σ_M^2 is just 0. One can see that when the arrival rate is fixed, delays will increase with its variability.

Our results can be seen in Figure 3. On the x-axis, we plot the system usage $\rho = \lambda/\mu$. Average delay is plotted on the y-axis. The two almost identical curves are M/G/1 and M/D/1 delay predictions (bold and dashed curve); i.e Poisson arrival with general and deterministic service. As a comparison, a classical Markovian queue (M/M/1) queue is also displayed (pointed curve). The reason why the two general queues predict lower delays than the Markovian queue is that the metering constraint of 10 NM is almost constant (we measured a squared coefficient of variation of $C_v^2 = \frac{\sigma_M^2}{\mu(M)^2} = 0.02$).

The delays depend on the average speed and spacing at the sector entry $(\bar{v}_{in}, \bar{s}_{in})$ and at the metering point $(\bar{v}_M, \bar{s}_M)$. The dimensionless system usage is then: $\rho = \frac{\lambda}{\mu} = \frac{\bar{v}_{in}}{\bar{s}_{in}} \frac{\bar{s}_M}{\bar{v}_M}$. This means that for an alternative inflow speed $\bar{v}'_{in}$ or a new metering constraint $\bar{s}'_M$, $\frac{\rho'}{\rho} = \frac{\bar{v}'_{in}}{\bar{v}_{in}} = \frac{\bar{s}'_M}{\bar{s}_M}$. Thus, the change of the demand/capacity ratio with inflow speed and metering minima is proportional. Accordingly, for the inflow spacing and the outflow speed, the impact on system usage is indirect proportional. In the figure, the dotted black line is the current demand/capacity ratio $\hat{\rho} = 0.53$. The theoretical average metering delay is 0.96 min The dotted red lines correspond to $\pm 10\%$ system usage modifications.

We conclude that in our context, Markovian arrivals with either general service or constant service generate similar theoretical average delays. Generalizations to arbitrary arrivals gets more complicated, and is initiated in [9].

Table 2: Nominal crossing times per route (radar data).

Route	crossing time (min)	$\hat{w}_{trk}$ (min)	N
W1	15.4 (2.2)	1.5	196
W2	14.7 (0.8)	1.1	894
W3	15.3 (0.9)	0.9	449
W4	14.4 (0.6)	1.0	713
W5	15.5 (0.8)	0.7	256
W6	15.4 (0.8)	0.9	286
Total	15.1 (1.0)	1.0	2794

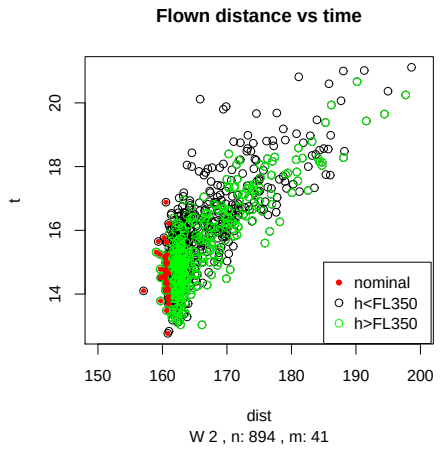

Figure 4: Distance vs. time for route W2.

3.2 Empirical Metering Delays

In order to estimate metering delays, we need to know the estimated times of arrival of each aircraft. One way to obtain them is to compare the time, that aircraft need to reach their destinations without metering delay with the actual time. We call the former the *nominal crossing time* and the latter the *observed crossing time*.

In this study, we compared two sources for the nominal crossing times:

- flight plan data: A flight plan is a sequence of waypoints and time-points $(wp_1, t_1), ..., (wp_n, t_n)$ indicating the desired trajectory from take-off (wp_1) until arrival (wp_n). The flight plan is submitted by the airline company several hours prior to the departure. This means that it is possible to take into account the weather conditions and aerodynamic parameters, such as the weight of the aircraft. A disadvantage of flight plan information is its low precision (its time resolution is in the unit 'minute').
- radar data: Radar data is available in the form $(t, lon_t, lat_t, h_t, id)$, where t is a time-stamp, lon_t, lat_t, h_t the position of the aircraft at time t and id a unique aircraft identifier. The time step between successive radar data observations is 10 seconds. We extracted for every route through T09 the distance flown and time required by the aircraft. Those with the shortest length were considered as the nominal crossing times. A disadvantage of this approach is that aircraft of different performance type and nominal crossing times under varying wind conditions are grouped together.

Table 3: Average metering delays.

Origin	$\hat{w}_{fp}$	$\hat{w}_{trk}$
Central (red)	1.4 (1.8)	1.1 (1.3)
South (yellow)	1.8 (2.1)	1.0 (1.1)
Int'l (green)	2.1 (1.7)	0.8 (1.0)
Total	1.6 (2.0)	1.0 (1.2)

Before presenting the results, a word on the data accuracy seems necessary. It turned out that in the flight plan data, a large number of flights had negative delay, meaning that they used less time than predicted to cross T09. As stated above, this suggests that the flight plan information is inaccurate. We set negative delays to the value 0 in this study. As far as the radar data is concerned, Figure 4 shows an example of one of the six routes, that we called W2, where the observed crossing times are plotted against the flown distances inside sector T09. One can see a cluster of points in the range 160-170 NM, taking between 13.5 and 16 minutes, and a branch with growing distance and crossing times. The red points mark the shortest paths, where no vectors occurred. We verified the selection graphically, by plotting the corresponding lateral and vertical trajectories. The green points mark trajectories on a flight level higher than FL 350. No pattern can be seen, concerning altitude. For all six routes, the nominal crossing times and the resulting empirical metering delays are summarized in Table 2. One can see that the crossing times lie between 14 and 15 minutes with standard deviations between 0.6 and 0.9 min (column 2). Route W1 has a higher standard deviation but also a lower sample size (column 4). Column 3 shows the resulting empirical average metering delays $\hat{w}_{trk}$. Compared to the crossing times, the standard deviations are below 10 %. But compared to the delays, these uncertainties are large enough to double the estimated metering delay of a given flight. The reasons for these high standard deviations are the aircraft performances and the wind conditions: in the winter months, a stronger west wind makes the aircraft fly faster than during the summer. With more data, we expect smaller standard deviations, but a more detailed estimation of the estimated times of arrival, for example with a trajectory prediction model, is necessary for more accurate results.

Having this said, the delay histograms can be seen in Figures 5 and 6. The colors represent the fraction of aircraft from the corresponding flows with a given delay. Both distributions are in the range of 0 to approximately 7 minutes. They both drop sharply with increasing delays. The black lines are the simulated delay distribu-

Table 4: Delay frequencies per region.

Origin \ Delay (min)	[0,1]	]1,2]	]2,3]	]3,4]	]4-5]	]5-6]	> 6
Central	0.60	0.22	0.10	**0.05**	**0.02**	0.01	~ 0
South	0.60	0.23	0.11	**0.04**	**0.01**	0.01	~ 0
Simu	0.69	0.17	0.08	0.03	0.02	0.01	~ 0

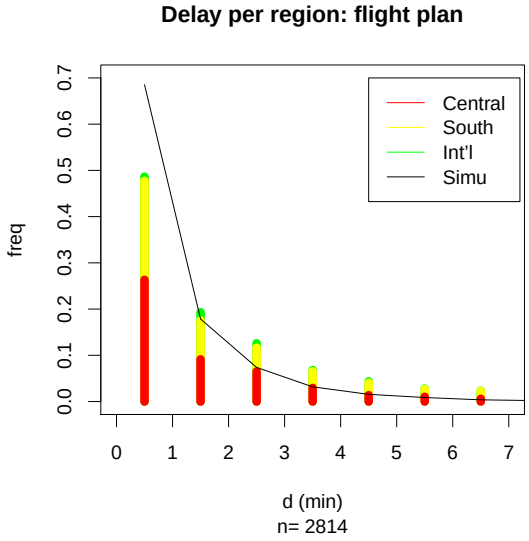

Figure 5: Empirical Metering Delay. Flight plan.

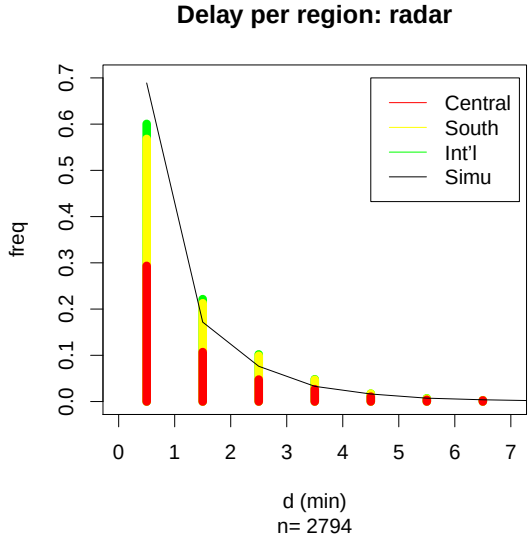

Figure 6: Empirical Metering Delay. Radar data.

tions of a queuing model with exponential inter-arrivals and deterministic service at 10 NM. The parameters were $\lambda = 0.32$ (min^{-1}) and $\mu = 0.61$ (min^{-1}), as we estimated in section 2. These models slightly under-predict the observed delays, except the smallest ones. This is expected because in reality, separation sometimes exceeds 10 NM, for example when a following aircraft has a higher ground speed than its leading aircraft.

The delay probabilities for the two flows (Central Japan and South Japan) are illustrated in Table 4. One can see that the distributions are equal in the intervals [0,1] and]5,6] min. But the delay frequencies for the flow from Central Japan (row 1) are slightly higher for the delays between 3 and 5 minutes (0.05 vs. 0.04 and 0.02 vs. 0.01) than in the flow from South Japan (row 2). A reason for this is that certain routes allow for more vectoring than others and that aircraft from Central Japan arrive more frequently on these routes than aircraft from the South. Compared with the simulated delays of a Poisson-Deterministic queue (row 3), an under-prediction of delays, except for the smallest ones, can be seen.

The average delays inside T09 are compared in Table 3. The delays based on flight plan information $\hat{w}_{fp}$ are 1.4, 1.8 and 2.1 minutes for the three regions (Central, South, Int'l), respectively. Their standard deviation are about 2 minutes (column 1). The delays based on radar data $\hat{w}_{trk}$ are throughout lower: 1.1, 1,0 and 0.8 minutes for the three regions with standard deviations about 1 minute (column 2). The total average on flight plan information is 1.6 minutes, whereas the total average on radar data is 1.0 minutes. For comparison with the theoretical delays: a queue with Poisson arrival and deterministic service (10 NM) would generate 0.95 minutes of average delay. Since theoretical delays are the minimal delays, observing that the radar delay is about 5 % higher than the queueing delay is not surprising.

We conclude the section on metering delays that (i) a simple queueing model captures the essential characteristics of the observed metering delays, (ii) that the flows from the different regions have slightly different delay patterns, depending on the routes they generally use, and (iii) that the radar data seems more accurate than the flight plan data,

4. OUTLOOK ON TRAFFIC SYNCHRONIZATION

In the future, trajectory-based operations (TBO) promise more accurate executions of planned flights [10, 11]. The common picture then is to identify the

Table 5: Required airspace and time for speed control.

Origin	v_{in} **(kt)**	$\hat{w}$ **(min)**	**s (NM)**	**tc (min)**	**airborne (min)**	**ratio**
Central	484 (39)	1.1 (0.75)	79.9 ± 65.3	11 ± 7.5	23.3 (6.0)	47.8 %
South	507 (39)	1.0 (0.75)	76.1 ± 67.3	10 ± 7.5	44.2 (3.2)	22.7 %
Int'l	522 (35)	0.8 (0.75)	62.6 ± 66.9	8 ± 7.5	59.1 (20.3)	13.6 %

times, at which aircraft should cross certain points in the airspace, such that the flows become more regular. ICAO calls this concept 'traffic synchronization', and characterizes it as a tactical flow measure because it takes place in the shortest of the flow management time horizons [2].

The simplest traffic synchronization strategy is speed control during the cruise phase, creating low additional workload for controllers and the crew. When t_i is the time to fly a distance s at speed v, and t_{ki} is the time at reduced speed kv $(0 < k < 1)$ then the required delay $w = t_{ki} - t_i = \frac{s(1-k)}{kv}$. Thus, the required distance to absorb w minutes of delay at reduced speed kv is $s = \frac{kvw}{1-k}$. Accordingly, aircraft i will reduce its cruise speed $tc = s/kv = w/(1-k)$ minutes before the sector entry. In reality, pilots will use the flight management system (FMS) to follow their optimized speed profiles. As stated in the introduction, a traffic management coordinator needs to know roughly how much delay to expect and how to distribute it in the airspace. This justifies the simplification in our study.

The major uncertainties in our measurements were the speed variations and the empirical delays. Minor uncertainty factors include the position errors of the radar data and the quantization error in the data recording. For the speed variations, we had standard deviation of around 39 kt in the three regions. The empirical delays depended on the nominal trajectories. In our measurements, the standard deviations of the sector traversal times of the nominal trajectories were between between 0.6 and 0.9 min per route (see Table 2).

Taking these uncertainties into account, we calculated the average distances and times for speed control at a speed reduction of 10 % for the delay values obtained in the previous section. The results can be seen in Table 5. For example, allowing for uncertainties in the range of one standard deviation, the flow from Central Japan (row 1) has an average arrival ground speed of 484 kt, with a standard deviation of 39 kt (column 2). Its average metering delay is 1.1. min, with an estimation error of $\pm$ 45 sec which we selected as an average of the measured uncertainties (column 3). In order to absorb this delay, an average required distance of 79.9 NM $\pm$ 65.3 NM , or equivalently 11 min $\pm$ 7.5 min of reduced speed prior to the estimated time of arrival at the sector entry are necessary (columns 4,5). The average airborne time of the flow is 23.3 min with a standard deviation of 6 min (column 6). Thus, aircraft would have to fly at reduced cruise speed for almost 50 % of the time (column 7). Better ratios are obtained for the flows from South Japan and international, with 22.6 % and 13.5 % respectively.

Clearly, the current uncertainties in the delay estimation are unsatisfactory. In the future, precise trajectory predictions are necessary to evaluate the concept and limitation of en-route trajectory control. Based on our estimations, we can conclude that the flows from Kyushu and International have a chance to be controlled by speed control. For the flow from Central Japan, precise flight management systems will be necessary (allowing speed control during climb), or more complex speed control, including en-route vectoring, or a better balance between ground delays and en-route delays will be necessary. All this is currently under study, see for example [9].

5. CONCLUSIONS

In this paper we analyzed metering delays in a Japanese arrival flow. The purpose of the analysis was to quantify them. Based on this, we discussed a strategy to absorb metering delays during the cruise phase instead of the descent phase as it it today's practice. Our main results were (i) a good correspondence between a queueing model and empirical data, (ii) low average delays, and (iii) high prediction uncertainties of sector crossing times. The results indicate that the traffic flows from South Japan and International are candidates for en-route speed control, while for the flow from Central Honshu, a balancing strategy between ground and en-route delay might be useful.

ACKNOWLEDGMENTS

The authors are grateful to the Japan Civil Aviation Bureau of the Ministry of Land, Infrastructure, Transport and Tourism for their cooperation in the provision of the data.

References

[1] M. S. Nolan. *Fundamentals of Air Traffic Control. Third edition*. Brooks/Cole, Wadsworth, 1998.

[2] ICAO. *Global Air Traffic Management Operational Concept*. International Civil Aviation Organization, 2005.

[3] S. Nagaoka. ENRI's R&D Long-term Vision. In *Proceedings of the ENRI International Workshop on ATM/CNS (EIWAC). Tokyo. Japan*, 2009.

[4] K. Kageyama and Y. Fukuda. A data analysis framework for delay studies on aircraft operational phases. *Proceedings of the 26th Congress of the International Council of the Aeronautical Science (ICAS). Anchorage, U.S.*, Oct. 2008.

[5] Multi Center Traffic Management Advisor Publication List. *http:// www.aviationsystemsdivision.arc.nasa.gov/ publications/ terminal/ mctma/ index.shtml*.

[6] G. Slater and D. Yang. Dynamic optimization of delay distribution in an uncertain environment. In *Proceedings of AIAA Conference on Guidance, Navigation, and Control (GNC2004). Providence, Rhode Island, USA*, 2004.

[7] R. W. Wolff. *Stochastic Modeling and the Theory of Queues*. Prentice-Hall, New Jersey, 1989.

[8] W. Feller. *An Introduction to Probability Theory and Its Applications, Volume 2*. Wiley, 2nd edition, 1970.

[9] C. Gwiggner and S. Nagaoka. On required distances to absorb metering delays. *Proceedings of the 2nd CEAS European Air & Space Conference. Manchester, U.K.*, 2009.

[10] Sesar Consortium. *The ATM Target Concept. D3*. The Sesar Consortium, 2007.

[11] Joint Planning and Development Office. *Concept of Operations for the Next Generation Air Transportation System*. Version 2.0, 2007.